Design and optimization of compact spot-size converters for silicon photonic devices

B. M. Azizur Rahman*[a], Weifeng Jiang[b]
[a]Department of Electrical and Electronic Engineering, City, University of London, Northampton Square, London EC1V OHB, UK; [b]College of Electronic and Optical Engineering, Nanjing University of Posts and Telecommunications, Nanjing 210023, China
*B.M.A.Rahman@city.ac.uk

ABSTRACT

The coupling between a silicon nanowire (NW) and a single mode fiber (SMF) is challenging. Design and optimization of compact spot-size converters (SSCs) for silicon photonics devices are presented by using numerically efficient and rigorous full-vectorial finite-element based approaches. The multi-Poly-Silicon layers based SSCs are proposed and optimized for the quasi-TE and quasi-TM polarizations sequentially. The coupling losses can be reduced to 2.72 dB and 2.45 dB for the quasi-TE and quasi-TM polarizations, respectively by using an eleven Poly-Si layers based SSC. A polarization-independent SSC is also proposed based on the phase-matched multi-Poly-Silicon layer and lower taper waveguide for both the quasi-TE and quasi-TM polarizations. Coupling to a lensed fiber with the radius of 2 μm, the optimized polarization-independent SSC is with the coupling losses of 0.34 and 0.25 dB for the quasi-TE and quasi-TM polarizations, respectively. The on-chip integrated SSC opens up the feasibility of a low cost passive aligned fiber-pigtailed electronic-photonics integrated circuits platform.

Keywords: Silicon photonics, spot-size converter, multi-layer, FEM, LSBR

1. INTRODUCTION

Silicon photonics has attracted attention as a promising technology for optical telecommunications and large scale photonic integrated circuits (PICs) [1]. Using highly sophisticated Complementary-Metal-Oxide-Semiconductor (CMOS) compatible process, silicon photonics fabricated on Silicon-On-Insulator (SOI) substrate would provide us with an inexpensive highly integrated photonic platform, in which ultra-compact photonic circuits can be achieved due to a very high index contrast. The major issues in wide spread use of silicon photonics are lack of any practical silicon based lasers, efficient modulators and coupling structures [2-4]. Additionally, in spite of progress in developing on-chip laser sources and modulators in silicon photonics, at present practical approaches require coupling light into and out of silicon devices. Particularly difficult is the coupling of light from a silicon nanophotonic waveguide to a standard optical fiber due to the large mode mismatch [5].

To achieve a high coupling efficiency between the silicon waveguide and optical fiber, various coupling schemes have been proposed recently. One approach could be the use of lenses, either bulk-optic lenses or a lensed fiber [6]. However, lenses require multiple anti-reflection (AR) coatings and complicated rigid packaging. Also, disadvantages of using lensed fiber are of critical fabrication process and small alignment tolerance. Another approach could be the use of a grating structure to couple light from an SOI waveguide into a fiber, which has the advantage of not requiring polished facets for coupling [7]. But, a grating-based coupling is inherently limited in spectral bandwidth, which also needs a vertical/tilted fiber-alignment. Another approach is to integrate a taper based spot-size converter (SSC) into the PIC system [8]. A 3D taper structure can adiabatically transform the mode of an SOI waveguide to the fiber mode [9]. Nevertheless, the fabrication of such taper requires gray scale lithography, which is not compatible with the standard CMOS process. An inverted taper using CMOS technology can make an adiabatic taper structure, while requires a thick buried oxide layer. Furthermore, the taper based SSC often has inherent loss, which is limited by the taper end-face reflection and radiation losses. Therefore, the efficient coupling of the silicon nanophotonic waveguide into optical fiber remains a challenge.

Here, we report a multi-layer based SSC without a taper for coupling between a silicon nanowire (NW) and a standard SMF, which can be easily fabricated by using standard CMOS process. In this case, a rigorous **H**-field based full-vectorial

finite element method (VFEM) is used to find the vector modes and supermodes of the coupled structure [10]. Following that, the least squares boundary residual (LSBR) method is used to find the power transfer efficiency and the coupling loss, which is a very rigorous approach particularly useful for non-identical and strongly coupled waveguide structure [11]. The present approach is fully vectorial in nature and being rigorous, will be as accurate as a full-vectorial 3D beam propagation method (BPM) approach, but computationally more efficient than the BPM.

2. THEORY

The **H**-field based VFEM has been used to find the modal field profiles at each segment of the multi-layer based SSC, which is one of the most accurate and efficient approaches. It is of great importance to accurately calculate the isolated mode and supermode profiles for both quasi-TE and quasi-TM polarized modes, subsequently used for calculating the power transfer efficiency, for designing a polarization-independent SSC. As for the cross-section of a multi-layer with a complex boundary, the **H**-field components are naturally continuous across the dielectric interfaces which can provide the most rigorous VFEM to characterize nonidentical and strongly coupled waveguide. The full-vectorial formulation is based on the minimization of the following energy functional [10]:

$$\omega^2 = \frac{\iint \left[(\nabla \times \mathbf{H})^* \cdot \varepsilon^{-1} (\nabla \times \mathbf{H}) + p (\nabla \cdot \mathbf{H})^* (\nabla \cdot \mathbf{H}) \right] dxdy}{\int \mathbf{H}^* \cdot \mu \cdot \mathbf{H} dxdy} \tag{1}$$

where ω^2 is the eigenvalue, **H** is the full-vectorial magnetic field, * denotes a complex conjugate and transpose, p is a weighting factor for the penalty term, ε and μ are the permittivity and permeability, respectively.

In this case, the LSBR method has been used to accurately calculate the supermode coefficient and power transfer efficiency for the multi-layer based SSC, consisting of two nonidentical waveguides. The LSBR method has been proved to be a powerful approach for nonidentical and strongly coupled waveguide structures. For a strong discontinuity interface, such as the end of the SSC and a SMF interface, the LSBR method can be used to estimate both the transmission and reflection coefficients by imposing the continuity of the transverse electric and magnetic fields at the junction interface in a least-squares sense. The LSBR method looks for a stationary solution to satisfy the continuity conditions in a least squares sense by minimizing the error energy functional, J, as given by [11]

$$J = \int \left| E_t^I - E_t^{II} \right|^2 + \alpha \cdot Z_0^2 \left| H_t^I - H_t^{II} \right|^2 d\Omega \tag{2}$$

where E_t^I, H_t^I and E_t^{II}, H_t^{II} are the transverse electric and magnetic fields in sections I and II, respectively. Z_0 is the free-space impedance, Ω is the junction interface, and α is the dimensionless weighting factor to balance the electric and magnetic components of the error functional J.

3. RESULTS

3.1 SSC for TE polarization

In this section, the coupling between a silicon NW and an SMF by using the proposed multi-layer based SSC is studied for the quasi-TE polarization. We propose one-layer and eleven multi-Poly-Si layers based SSCs for the quasi-TE polarization. The coupling schematic of the proposed SSC is shown in Figure 1(a), consisting of a multi-layer based SSC between a silicon NW and an SMF [12]. The coupling length is denoted by L. The cross-section of the multi-layer based SSC is shown in Figure 1(b). The lower silicon NW is with the size of w_1 × H. The upper waveguide is comprised of the multi-Poly-Si and silica layers with the thicknesses of h and S_p, respectively. The width of the upper multi-layer is denoted by w_2. The gap between the lower and upper waveguides is denoted by S. In this paper, the refractive indices of the silicon, Poly-Si, and silica are set to be 3.47548, 3.48, and 1.46, respectively at 1550 nm. The size of the lower silicon waveguide is chosen to be w_1 × H = 400 nm × 220 nm. The width of the upper waveguide is chosen to be 6 μm to expand its spot-size horizontally.

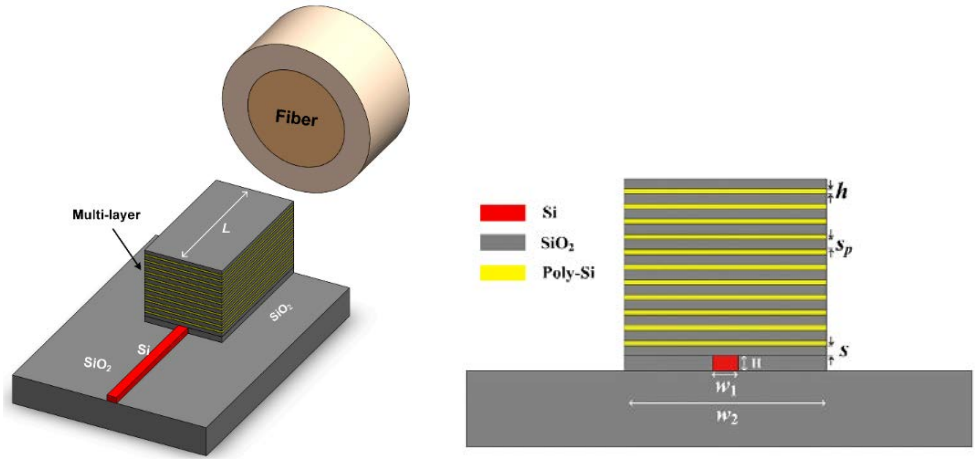

(a) (b)

Figure 1. Schematic of the proposed SSC: (a) Schematic diagram for coupling process, (b) Cross-section of the SSC.

In this section, the number of the upper Poly-Si layers is sequentially set to be one and eleven to expand its spot-size vertically. Firstly, the analysis for a single-Poly-Si layer based SSC is presented. The effective index (n_{eff}) for the fundamental TE mode of an isolated Poly-Si layer is calculated by varying the height, h. A single layer of wider Poly-Si can be phase matched to silicon NW. Variations of n_{eff} with the height of the Poly-Si layer, h, for the H_y^{11} mode are shown in Figure 2. It can be observed that as the height, h, of the Poly-Si layer is increased, the n_{eff} of the H_y^{11} mode is increased. The n_{eff} of the isolated Poly-Si layer becomes equal to the n_{eff} of the silicon NW without upper layer when h = 107 nm as the two curves cross each other and in this case phase matching between the isolated wider Poly-Si layer and silicon NW can be achieved.

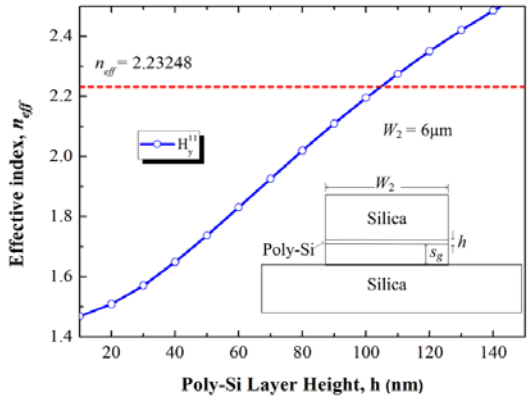

Figure 2. Variations of n_{eff} with the height of the Poly-Si layer, h, for the H_y^{11}mode. The horizontal line represents the n_{eff} of the silicon waveguide without the upper layer.

Although the phase-matching condition was determined with isolated mode analysis, it is necessary to it is necessary to study the supermode characteristics for the proposed SSC due to the strong mode-coupling effect. In order to get the phase-matching condition, variations of the propagation constants of the even and odd supermodes with the height of the Poly-Si layer are calculated by using the VFEM and shown in Figure 3(a). It can be noted that two curves become closest at the phase-matching point, which would get mix-up and form even and odd supermodes. The curves for S = 300 nm are closer than that for S = 500 nm due to the stronger mode-coupling effect. The coupling lengths for these two gaps are also calculated based on $L_c=\pi/(\beta_{even}-\beta_{odd})$, where β_{even} and β_{odd} are propagation constants of the even and odd supermodes, respectively [12]. Variations of the coupling lengths with the height of the Poly-Si layer are shown in Figure 3(b). It can be noted that a more compact length would be obtained with a narrower gap. The curve for S = 300 nm is more flat compared with S = 500 nm, which reveal that it is more insensitive to the change of the height of the Poly-Si layer.

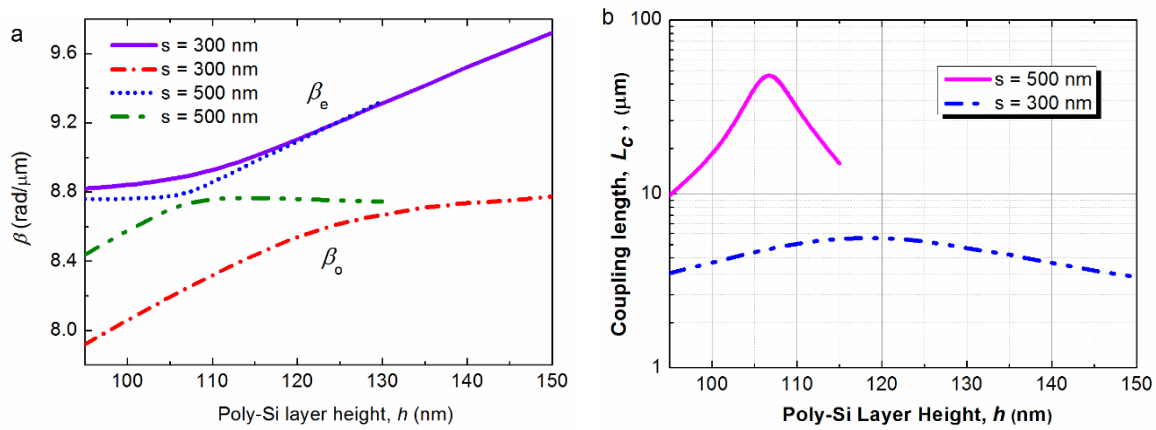

Figure 3. Coupling characteristics of single-layer based SSC. (a) Even and odd supermode β variations with Poly-Si height (h) for S = 300 nm and 500 nm, respectively. (b) Variations of coupling length, L_c with h for S = 300 nm and 500 nm, respectively.

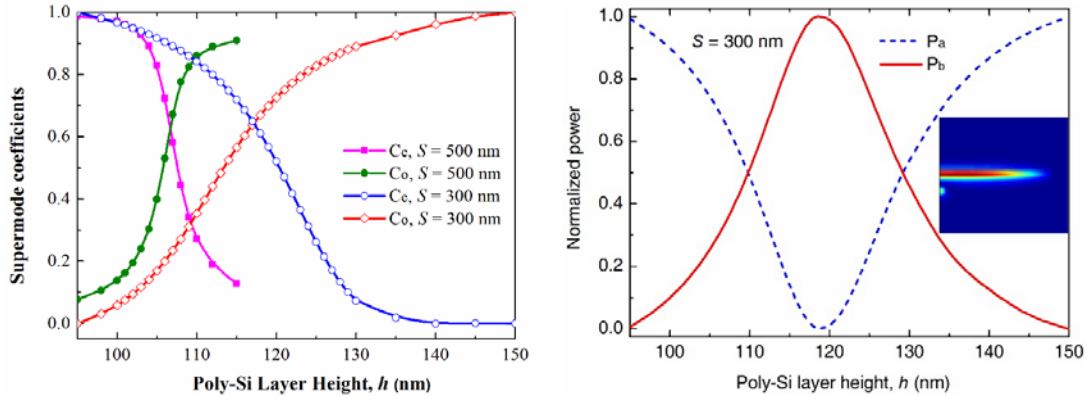

(a) (b)

Figure 4. (a) Variations of even-like and odd-like supermode coefficients with h for S = 300 and 500 nm, respectively. (b) Variations of the normalized power transfer efficiency with h for S = 300 nm. The inset is the output modal field at z = L_c. P_a and P_b are the power in the Poly-Si layer and the silicon NW, respectively.

For weakly coupled identical waveguides, the amplitudes of two supermodes can be equal when an incident wave launched into any of the two waveguide. However, for the strongly coupled and/or non-identical waveguides, the coefficients of two supermodes may not be equal, which can cause incomplete transfer of power and increase of the crosstalk. Especially, the supermode coefficients could be highly unequal for non-identical waveguides when they are not phase matched. To study the phase matching for the two non-identical coupled waveguides, the supermode coefficients for the even-like and odd-like supermodes are calculated by using the LSBR method. Variations of even-like and odd-like supermode coefficients (C_e and C_o) with h for S = 300 and 500 nm, respectively, are shown in Figure 4(a). The pink and green lines are shown for the even-like and odd-like supermode coefficients of the SSC with the separation, S = 500 nm. The blue and red lines are shown for the even-like and odd-like supermode coefficients of the SSC with the separation, S = 300 nm. For both separations, it can be noted that as the height of the Poly-Si layer is increased, the coefficient of the even-like mode (C_e) is monotonically reduced, whereas the coefficient of the even-like mode (C_o) is monotonically increased. It can be observed that for S = 500 nm, both supermode coefficients have value of 0.64 near the phase matching for isolated waveguides with h = 107 nm, in which the value is nearly equal to $1/\sqrt{2}$, and so each supermode carries approximately half of the total power. When the height of the Poly-Si layer is far away from the phase matching, the two supermode coefficients are considerably different. As shown in Figure 4(a), for S = 300 nm, both supermode coefficients have values of 0.65 and 0.63, respectively, near the phase matching for the composite waveguide with h = 117 nm, in which the value is also nearly equal to $1/\sqrt{2}$, and the supermode can carry approximately half of the total power. In order to reduce the coupling length, the separation, S, is chosen as 300 nm for the single layer based SSC to coupling with the SMF. For the separation S = 300 nm, when the necessary phase matching can be achieved the coupling length is only 5.5 μm. Finally, the power transfer

efficiency is calculated by using the LSBR method and shown in Figure 4(b). P_a and P_b are the power in the lower silicon NW and the power coupled to the upper Poly-Si layer, respectively. It can be noted from Figure 4(b) that under the phase-matching condition, the power transfer efficiency can achieve to be 93.2% from the lower silicon NW to the upper Poly-Si layer. The coupling efficiency between the single-layer based SSC and the SMF is calculated to be 21.6%, while that for the direct coupling is only 3.9%.

In order to further increase the coupling efficiency between the multi-layer based SSC and the SMF, an eleven-Poly-Si layer based SSC is considered. Phase-matching conditions between the upper isolated eleven-Poly-Si layers and lower silicon NW are shown in Figure 5(a). It can be noted that the phase-matched height is increased with the increase of the height of the upper silica layer. In order to maximize the effective area (A_{eff}) of the upper waveguide core, variations of effective area A_{eff} with S_p for the even modes at phase matching points for half structure of the eleven Poly-Si layers are calculated by using the VFEM and shown in Figure 5(b). It can be noted that the maximum A_{eff} of the upper waveguide can be achieved to be 44.8 μm^2 for S_p = 400 nm and h = 95.0 nm. The corresponding field profile (H_y field) is shown in Figure 5(b) as an inset.

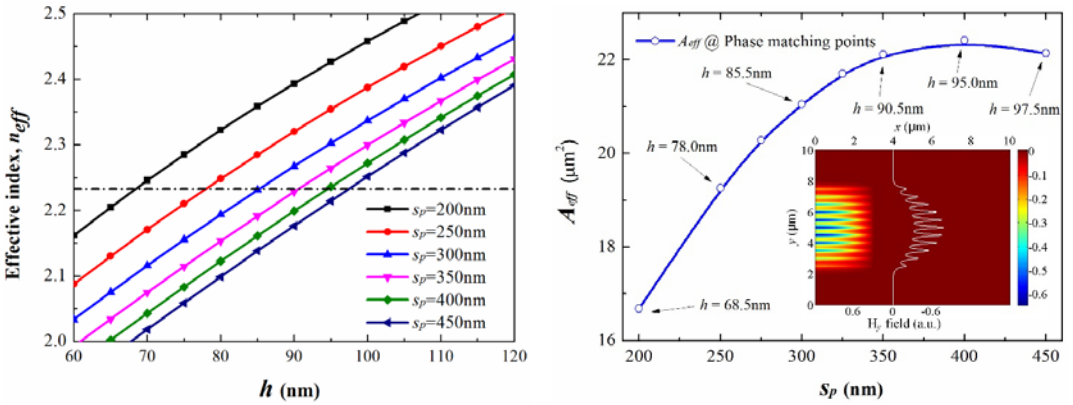

Figure 5. (a) Phase-matching conditions for isolated eleven-Poly-Si layers. (b) Variations of effective area A_{eff} with S_p for the even modes at phase matching points for half structure of the eleven Poly-Si layers. The inset is the field profile of the isolated layers for maximum A_{eff}.

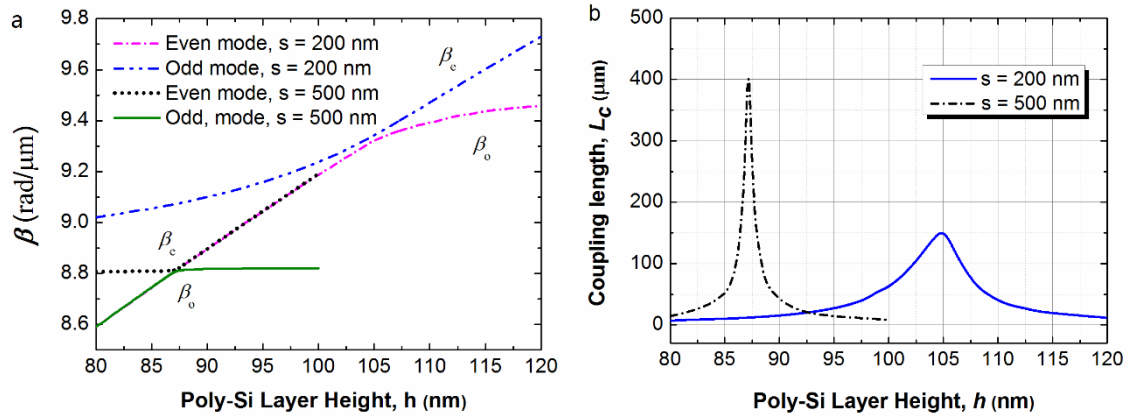

Figure 6. Coupling characteristics of the eleven layers based SSC. (a) Even and odd-like supermode β variations with Poly-Si Height (h) for S = 200 nm and 500 nm, respectively. (b) Variations of coupling length L_c with h for S = 200 nm and 500 nm, respectively.

The phase-matching condition for the combined structure is studied for the eleven-layer based SSC. Variations of propagation constants of the even and odd supermodes are shown in Figure 6(a). The phase-matched heights of the Poly-Si layer are calculated to be h = 105 and 87.2 nm for the gaps, S = 200 and 500 nm, respectively. The coupling lengths are also calculated and shown in Figure 6(b). Here, the gap, S = 200 nm is chosen for eleven-layer based SSC and the coupling length is calculated to be 158.67 μm. For the phase-matched height, h = 105 nm for the gap, S = 200 nm, the H_y field profiles of the even-like and odd-like supermodes are shown in Figure 7. It can be noted that these supermodes are not

strictly even- or odd-type since two guides were not identical. Although maximum amplitudes in the upper multi-layer array and the lower silicon NW are different as their core-sizes were also different, but nearly equal powers are distributed in two non-identical guides.

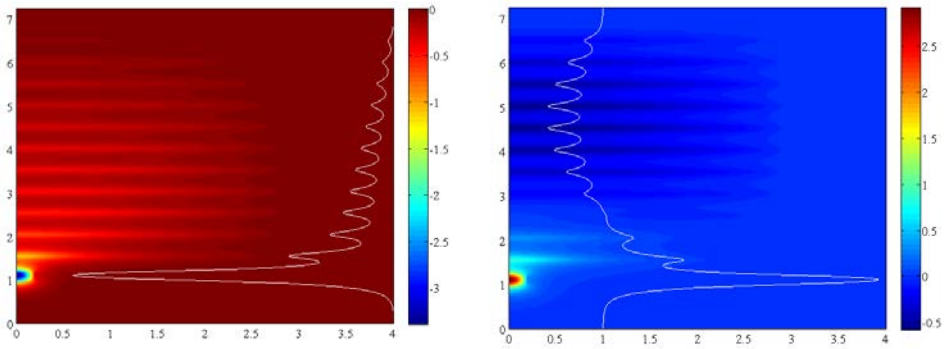

(a) (b)

Figure 7. H_y field profiles of the phase matched (a) even-like and (b) odd-like supermodes.

Finally, the power transfer efficiency between the lower silicon NW and upper eleven-layer based waveguide is calculated by using the LSBR method and shown in Figure 8. It can be noted that the power transfer efficiency is calculated to be 95.2% at the phase-matched height. The coupling efficiency between the eleven-layer based SSC and the SMF is calculated to be 56.1%. The total coupling loss is 2.72 dB from the silicon NW to the SMF and vice versa. In order to further increase the coupling efficiency, a lensed fiber with the radius of 2 μm, the core and cladding refractive-indices of 1.4731 and 1.45 is introduced. The coupling losses are reduced to be only 0.34 dB for coupling between the lensed fiber and eleven-layer based SSC.

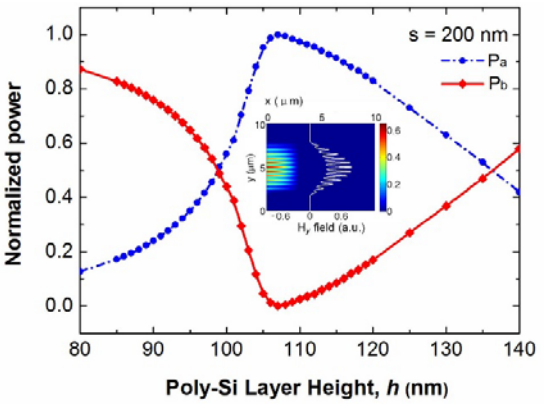

Figure 8. Variations of the normalized power transfer efficiency with h for S = 200 nm. The inset is the output modal field at z = L_c.

3.2 SSC for TM polarization

For the coupling between the on-chip silicon NW and SMF, it is important to provide an SSC not only for singular polarization but also for both the quasi-TE and quasi-TM polarizations. In this section, the optimization of the proposed SSC for the quasi-TM polarization is presented. In section 3.3, a polarization-independent SSC is given. Here, an eleven-layer based SSC is studied for the quasi-TM as an example. Similarly to the optimization process for the quasi-TE mode, Variations of effective area, A_{eff} with S_p for the even modes at phase matching points are shown in Figure 9(a). It can be noted that the maximum A_{eff} of 60 μm^2 can be obtained for S_p = 500 nm and h = 146.5 nm. The corresponding field profile of the isolated Poly-Si layers for the maximum A_{eff} at the phase matching point (S_p = 500 nm) is shown in Figure 9(b). The power transfer efficiency between the lower silicon NW and the upper multi-layers is calculated by using the LSBR method and shown in Figure 9(c). The coupling efficiencies are calculated to be 96.8% and 99.3%for the gaps, S = 500 and 800 nm, respectively. The coupling efficiency between the SSC and SMF is calculated to be 59.6%.

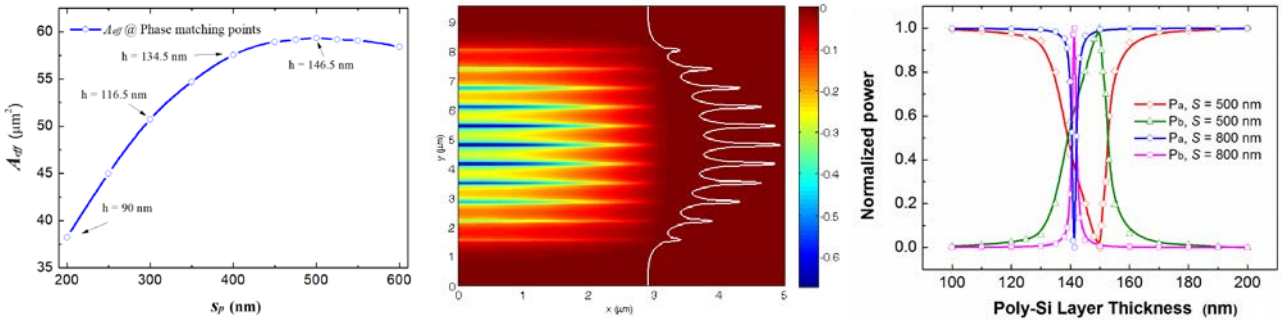

(a) (b) (c)

Figure 9. (a) Variations of effective area A_{eff} with S_p for the even modes at phase matching points. (b) Field profile of the isolated Poly-Si layers for the maximum A_{eff} at the phase matching point (S_p = 500 nm). (c) Variation of the normalized power transfer efficiency with t for S = 500 and 800 nm.

3.3 Polarization-independent SSC

In this section, a polarization-independent SSC is proposed as shown in Figure 10(a). It can be noted that the input quasi-TE mode can be completely coupling from the lower silicon NW to the upper multi-layer waveguide at the end of Section I. As the parameters of the upper multi-layer were determined in Section I, a taper silicon NW in Section II is introduced to change the width of the lower silicon NW, which can achieve the phase-matching condition for the quasi-TM mode in Section III. Hence, the input quasi-TM mode would propagate along the lower silicon NW and be transferred to the upper multi-layer waveguide at the end of Section III. Finally, a polarization combiner is introduced to combine the quasi-TM mode to the waveguide of the quasi-TE mode. The power transfer from the lower silicon NW to the upper multi-layer waveguide was given in Section 3.1 for the quasi-TE mode. Variations of the normalized power transfer efficiency with the width of the silicon NW are shown in Figure 10(b) for the quasi-TM mode. The power transfer efficiency of the quasi-TM is calculated to be 95.5% for the phased-matched width of W_1 = 225 nm. When coupling to a lensed fiber with the radius of 2 μm, the total coupling loss is calculated to be only 0.25 dB for the quasi-TM mode. In addition, the coupling efficiency can be further enhanced by adding the index-matching oil.

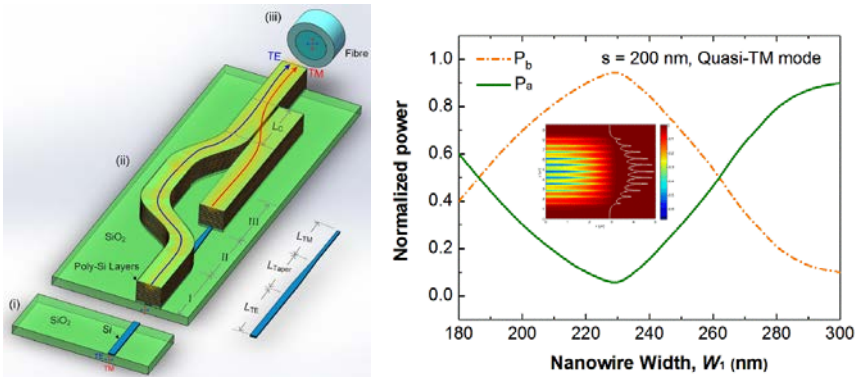

(a) (b)

Figure 10. (a) Schematic of polarization-independent SSC based on the multi-layer. (b) Variations of the normalized power transfer efficiency with the width of the silicon NW.

4. CONCLUSION

In conclusion, the concept of the multi-layer based SSC has been proposed and optimized for both the quasi-TE and quasi-TM polarizations. For identical waveguide and weak coupling, often coupled mode theory could be adequate to estimate power transfer between coupled waveguides. However, when coupling is strong, waveguides are non-identical and as in this case modes are highly hybrid, a full-vectorial rigorous numerical approach is necessary. The VFEM and LSBR method has been used to study the mode and propagation characteristics. The coupling losses were calculated to be 2.72 dB and 2.45 dB for the quasi-TE and quasi-TM polarizations, respectively by using an eleven Poly-Si layers based SSC. A

polarization-independent SSC has been proposed. The coupling losses were reduced to be 0.34 and 0.25 dB for the quasi-TE and quasi-TM polarizations, respectively, coupling to a lensed fiber with a radius of 2 μm.

5. ACKNOWLEDGEMENTS

This work was supported in part by the Erasmus Mundus INTACT Project, in part by the Natural Science Foundation of Jiangsu Province (Grant No. BK20180743), in part by the NUPTSF (Grant No. NY218108), and in part by the Research Center of Optical Communications Engineering & Technology, Jiangsu Province.

REFERENCES

[1] D. Thomson, D., *et al*., "Roadmap on silicon photonics," Journal of Optics 18(7), 073003 (2016).
[2] D. Liang, and J. E. Bowers, "Recent progress in lasers on silicon," Nat. Photon. 4, 511-517 (2010).
[3] E. Timurdogan, *et al*., "An ultralow power athermal silicon modulator," Nat. Commun. 5, 1-11 (2014).
[4] C. Kopp, S. Bernabe, B. B. Bakir, J. M. Fedeli, R. Orobtchouk, F. Schrank, and T. Tekin, "Silicon photonic circuits: on-CMOS integration, fiber optical coupling, and packaging, " IEEE J. Sel. Top. Quantum Electron. 17(3), 498-509 (2011).
[5] J. Cardenas, et al., "High coupling efficiency etched facet tapers in silicon waveguides," IEEE Photonics Technol. Lett. 26(23), 2380-2382 (2014).
[6] T. H. Loh, *et al*., "Ultra-compact multilayer Si/SiO_2 GRIN lens mode-size converter for coupling single-mode fiber to Si-wire waveguide," Opt. Express 18(21), 21519-21533 (2010).
[7] G. Roelkens, *et al*., "High efficiency diffractive grating couplers for interfacing a single mode optical fiber with a nanophotonic silicon-on-insulator waveguide circuit," Appl. Phys. Lett. 92(13), 131101 (2008).
[8] A. Khilo, M. A. Popović, M. Araghchini, and F. X. Kärtner, "Efficient planar fiber-to-chip coupler based on two-stage adiabatic evolution," Opt. Express 18(15), 15790-15806 (2010).
[9] N. Fang, *et al*., "Three-dimensional tapered spot-size converter based on silicon-on-insulator," IEEE Photonics Technol. Lett. 21(9), 820-822 (2009).
[10] B. M. A. Rahman and J. B. Davies, "Finite-element solution of integrated optical waveguides," J. Lightwave Technol. 2(5), 682-688 (1984).
[11] B. M. A. Rahman and J. B. Davies, "Analysis of optical waveguide discontinuities," J. Lightwave Technol. 6(1), 52-57 (1988).
[12] W. Jiang, N. Kohli, X. Sun, and B. M. A. Rahman, "Multi-poly-silicon-layer based spot-size converter for efficient coupling between silicon waveguide and standard single-mode fiber," IEEE Photon. J. 8(3), 6600612, (2016).